# Protease-Independent Production of Poliovirus Virus-like Particles in *Pichia pastoris*: Implications for Efficient Vaccine Development and Insights into Capsid Assembly

Lee Sherry,[a] Jessica J. Swanson,[a] Keith Grehan,[a] Huijun Xu,[a] Mai Uchida,[b] Ian M. Jones,[b] Nicola J. Stonehouse,[a] David J. Rowlands[a]

aAstbury Centre for Structural Molecular Biology, School of Molecular and Cellular Biology, Faculty of Biological Sciences, University of Leeds, Leeds, United Kingdom
bUniversity of Reading, School of Biological Sciences, Reading, United Kingdom

**ABSTRACT** The production of enterovirus virus-like particles (VLPs) that lack the viral genome have great potential as vaccines for a number of diseases, such as poliomyelitis and hand, foot, and mouth disease. These VLPs can mimic empty capsids, which are antigenically indistinguishable from mature virions, produced naturally during viral infection. Both in infection and *in vitro*, capsids and VLPs are generated by the cleavage of the P1 precursor protein by a viral protease. Here, using a stabilized poliovirus 1 (PV-1) P1 sequence as an exemplar, we show the production of PV-1 VLPs in *Pichia pastoris* in the absence of the potentially cytotoxic protease, 3CD, instead using the porcine teschovirus 2A (P2A) peptide sequence to terminate translation between individual capsid proteins. We compare this to protease-dependent production of PV-1 VLPs. Analysis of all permutations of the order of the capsid protein sequences revealed that only VP3 could be tagged with P2A and maintain native antigenicity. Transmission electron microscopy of these VLPs reveals the classic picornaviral icosahedral structure. Furthermore, these particles were thermostable above 37°C, demonstrating their potential as next generation vaccine candidates for PV. Finally, we believe the demonstration that native antigenic VLPs can be produced using protease-independent methods opens the possibility for future enteroviral vaccines to take advantage of recent vaccine technological advances, such as adenovirus-vectored vaccines and mRNA vaccines, circumventing the potential problems of cytotoxicity associated with 3CD, allowing for the production of immunogenic enterovirus VLPs *in vivo*.

**IMPORTANCE** The widespread use of vaccines has dramatically reduced global incidence of poliovirus infections over a period of several decades and now the wild-type virus is only endemic in Pakistan and Afghanistan. However, current vaccines require the culture of large quantities of replication-competent virus for their manufacture, thus presenting a potential risk of reintroduction into the environment. It is now widely accepted that vaccination will need to be extended posteradication into the foreseeable future to prevent the potentially catastrophic reintroduction of poliovirus into an immunologically naive population. It is, therefore, imperative that novel vaccines are developed which are not dependent on the growth of live virus for their manufacture. We have expressed stabilized virus-like particles in yeast, from constructs that do not require coexpression of the protease. This is an important step in the development of environmentally safe and commercially viable vaccines against polio, which also provides some intriguing insights into the viral assembly process.

**KEYWORDS** poliovirus, vaccine, virus-like particle, *Pichia pastoris*, poliomyelitis, vaccines

Poliomyelitis, a devastating paralytic and potentially fatal disease caused by poliovirus (PV) has been responsible for many global epidemics over the past century. The introduction of the Global Polio Eradication Initiative (GPEI) in 1988, has resulted in >99% reduction in

paralytic poliomyelitis cases globally and the goal of the initiative is to eliminate the virus (1). This reduction in paralytic PV cases has resulted from the widespread application of two vaccines: the live-attenuated oral PV vaccine (OPV) and the inactivated PV vaccine (IPV) (2). Vaccine deployment has also led to wild-type (wt) PV-2 and wt PV-3 being declared eradicated in 2015 and 2019, respectively, with only wt PV-1 still circulating in Afghanistan and Pakistan (3). As we near eradication, biosafety concerns surround both OPV and IPV as each requires large scale virus growth and thus has the potential to reintroduce the virus into the environment (2).

While IPV provides excellent humoral immunity, it induces little mucosal immunity and therefore does not prevent viral infection or transmission within a population (4). The contribution of OPV to the near-eradication of PV is immense, however, the attenuated virus can quickly revert to virulence, leading to vaccine-associated paralytic poliomyelitis (VAPP) and, in areas with low vaccine coverage, the spread of vaccine-derived PV (cVDPV) (5). Unfortunately, cVDPV cases now outnumber wt PV cases globally (1), furthermore, OPV can recombine with other PVs or PV-like enteroviruses to regain virulence (6, 7). However, the recent introduction of nOPV2 vaccine, which significantly decreases the likelihood of reversion and recombination, may help to reduce VDPV circulation and therefore assist in PV eradication (8).

PV belongs to species *Enterovirus C* within the picornavirus family of positive-sense RNA viruses and has a 7.5 kb genome. The majority of the genome encodes a large continuous open-reading frame (ORF), which is proteolytically processed after translation into mature protein products. In addition, a short upstream ORF (uORF) has recently been identified and shown to be important in *ex vivo* organoid infection by Echovirus 7 (9). The major ORF comprises 3 distinct regions; P1, which encodes the viral capsid proteins, and P2 and P3, which encode the nonstructural proteins. Proteolytic cleavage of the polypeptide by the viral proteases, $2A^{pro}$, $3C^{pro}$, and 3CD, occurs co- and posttranslationally, yielding the mature viral proteins required for viral replication (10). The viral protease precursor, 3CD, specifically cleaves P1 into the individual capsid's proteins, VP0, VP3 and VP1 (11, 12). A further maturation cleavage of VP0 into VP4 and VP2 is associated with encapsidation of viral RNA and results in enhanced particle stability (13, 14).

The mature PV virion is an ∼30 nm icosahedral capsid, comprised of 60 copies of VP1-VP4, containing the viral genome (15). During infection, particles lacking viral genome are also produced. These particles, termed empty capsids (ECs), are antigenically indistinguishable from mature virions, although VP0 remains uncleaved (16). Recombinant ECs have potential as virus-like particle (VLP) vaccines; however, wt ECs are inherently unstable and their antigenic conformation changes at lower temperatures than is the case for mature viral particles (16, 17). This conformational change results in a minor expansion of the particles but has significant consequences for their antigenicity. ECs readily convert from the native antigenic form (termed D-Ag) to the nonnative form (termed C-Ag). Although the D-antigenic form induces protective immune responses to PV, the C-antigenic form does not (17–19). Therefore, recombinant VLP vaccines against PV must retain the D-antigenic conformation.

VLPs are a safe and attractive option as recombinant vaccines as they mimic the repetitive structures of virions but lack the genome and are noninfectious. Both the hepatitis B virus (HBV) and human papillomavirus (HPV) vaccines are licensed VLP-based vaccines produced in yeast and insect cells, respectively (20–22). Following the initial demonstration of the expression of PV VLPs in yeast in 1997 (23), these have been produced in several systems in recent years, including mammalian, plant and insect cells (24–30). However, most of these systems rely on the coexpression of the viral protease, 3CD, to cleave the viral structural protein to produce VLPs. There are some concerns around the potential cytotoxicity of 3CD and its potential impact on VLP yield in recombinant systems. Additionally, 3CD has been shown to induce apoptosis in mammalian cells (31), which may limit the application of newly licensed vaccine technologies such as viral vectors and mRNA vaccine technologies to produce next-generation poliovirus vaccines.

We have previously demonstrated the production of PV VLPs using *Pichia pastoris* and modulated the expression of 3CD through a number of molecular approaches (30).

Interestingly, Xu et al. reported an insect cell expression system which yielded PV VLPs in the absence of the viral protease by splitting the P1 precursor protein across 2 ORFs, with VP3 and VP0 under the control of one promoter and separated by the porcine teschovirus 2A peptide (P2A), and VP1 under the control of a second promoter (28), which also changes the natural order of proteins on the P1 precursor, i.e., VP0-VP3-VP1.

Here, we investigated the potential for protease-independent VLP production in *Pichia pastoris*. We show that stabilized PV-1 VLPs (32) can be produced in *Pichia* without the viral protease, 3CD, using instead the P2A peptide sequence to terminate translation between individual capsid proteins, and compare this to protease-dependent production of PV-1 VLPs. Analysis of all permutations revealed that only VP3 could be tagged with P2A and maintain native antigenicity. Transmission electron microscopy of these VLPs reveals their classic picornaviral icosahedral structure. Finally, we show that these particles are thermostable above 37°C, demonstrating their potential as next-generation polio vaccine candidates.

## RESULTS

**Protease-independent production of poliovirus structural proteins.** Previously, we reported the production of PV VLPs in *Pichia pastoris* using dual promoter constructs to separately express P1 and the viral protease, 3CD. However, the overexpression of 3CD can be cytotoxic and may reduce the yield of PV VLPs in heterologous systems (30, 31). Xu et al. demonstrated production of protease-independent PV VLPs in native conformation in insect cells using recombinant baculoviruses to express the viral structural proteins under the control of two separate promoters, with VP3 and VP0 separated by P2A transcribed from the first promoter and VP1 under the control of the second promoter (Xu et al. 2019). The short peptide sequence 2A is present at the C terminus of the P1 region of aphthoviruses that interrupts translation to separate the P1 and P2 regions without proteolytic cleavage. Here, we undertook a detailed study of the protease-independent expression of PV-1 VLPs in *Pichia* using a matrix of constructs based on a PV-1 sequence which includes several stabilizing mutations (32) (Fig. 1A). We compared protein expression and VLP assembly from these constructs with the dual alcohol oxidase (AOX) promoter P1/3CD system we reported previously, together with a modified construct in which the VP1 sequence was extended at the C terminus with a 6xHIS tag.

*Pichia* colonies, transformed with each construct, were tested for the level of expression. Samples from small-scale expression were collected 48 h postinduction and analyzed for correct processing, either by 3CD or P2A, using an anti-VP1 antibody (Fig. 1B). All constructs produced VP1, albeit at different levels. Both protease-containing constructs, PV-1 SC6b P1 and PV-1 SC6b 6xHIS, and the protease-independent constructs in which VP1 was upstream of 2A or was produced from a separate promoter, produced readily detectable levels of VP1. However, in constructs where VP1 followed the P2A peptide, VP3-2A-VP1 VP0 (31-0) and VP0-2A-VP1 VP3 (01-3), respectively, the level of VP1 was markedly lower. This suggests that, although in an optimum context P2A can facilitate a 1:1 ratio of up- and downstream protein expression in mammalian cells, the surrounding sequence or the reinitiation event following 2A-mediated interruption of translation may influence the translation rates in *Pichia*. As expected, anti-3D reactivity was only seen with lysates of the protease-containing constructs, where two major bands were detected at approximately 72 and 55 kDa, respectively (Fig. 1B).

**VLPs produced from protease-dependent and independent constructs sediment similarly.** To determine VLP assembly competence of the protease-independent constructs, high-expressing *Pichia* clones of each were cultured to high-density and expression induced with 0.5% methanol (vol/vol) and cell pellets collected 48 h postinduction. The resuspended pellets were homogenized at ~275 MPa and the resultant lysates purified through chemical precipitation and differential centrifugation steps culminating in 15 to 45% sucrose gradients. With the exception of the VP0-2A-VP3 VP1 (03-1) construct, immunoblot analysis of gradient fractions detected VP1 in fractions consistent with the presence of VLPs (Fig. 2) with intensities that were broadly consistent with the total protein analysis (Fig. 1). Constructs in which 2A followed VP0 produced lower yields of VLPs suggesting a conformation incompatible with efficient assembly. Minor differences in peak fractions was also noted with those constructs containing VP1-2A or VP1-His trending to peak higher in the gradient.
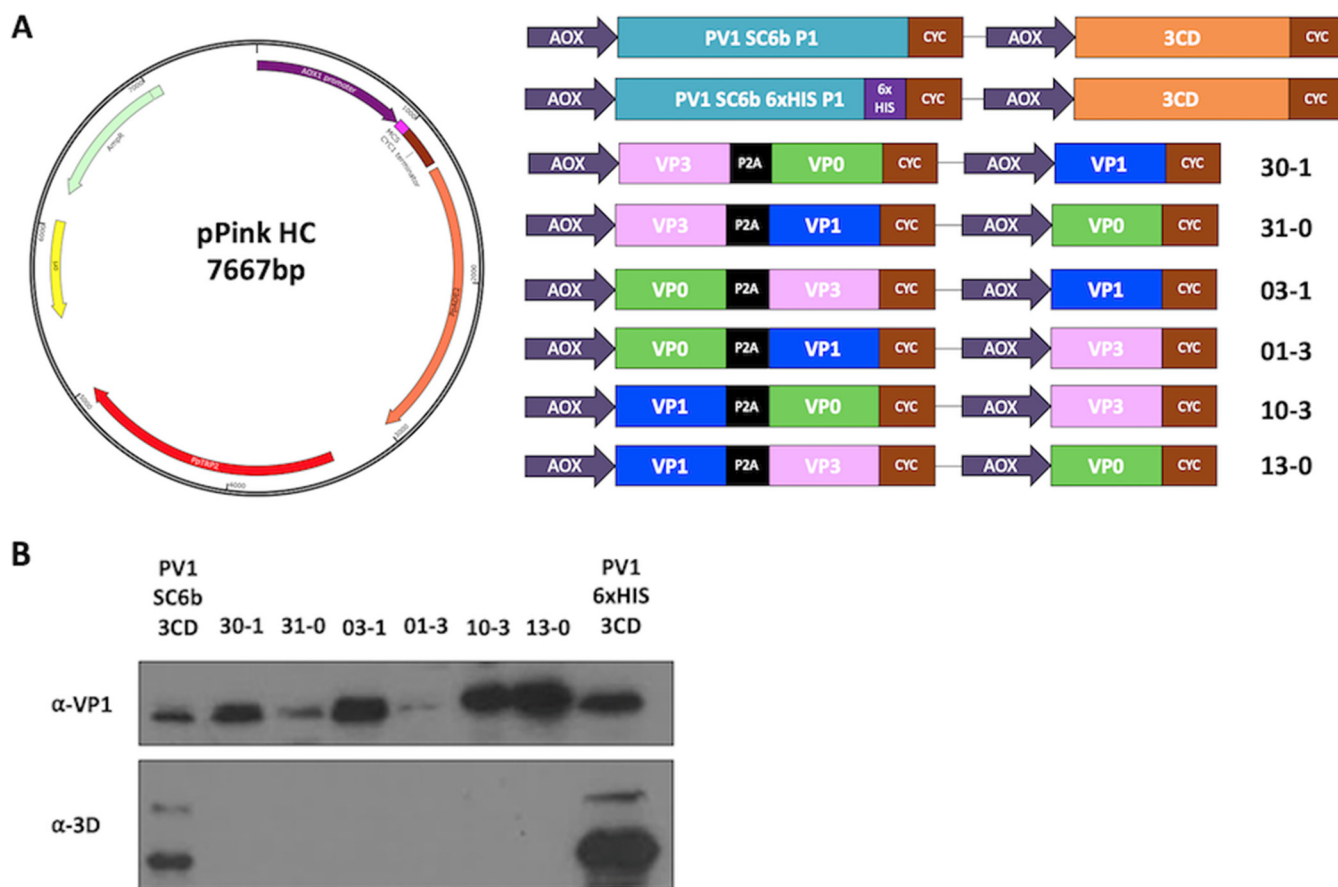
**FIG 1** Schematic of expression cassettes and immunblots. (A) The pPink HC expression vector with the dual alcohol oxidase (AOX) promoter expression constructs which drive the expression of the P1 capsid protein and the viral protease, 3CD or the expression of protease-free constructs with VP0 (green), VP3 (pink), and VP1 (blue). (B) Immunoblot for PV VP1 and 3D. Samples were collected 48 h postinduction and lysed using 0.1 M NaOH. All samples were boiled in 2x Laemlli buffer and separated by SDS-PAGE prior to analysis by immunoblot using mouse monoclonal $\alpha$-VP1 and rabbit monoclonal $\alpha$-3D antibody. The figure is a representative example of three separate experiments for each construct.

**VP3-P2A VLPs are D-antigenic.** To confirm the antigenicity of the VLPs, the peak fractions were analyzed by enzyme-linked immunosorbent assay (ELISA) using a standard protocol established by the National Institute for Biological Standards and Control (NIBSC) with the current inactivated vaccine standard (termed BRP) as a positive control (32). As expected, the PV-1 SC6 3CD produced both D and C antigenic VLPs, with the ratio of D:C largely in favor of D-antigenic particles (Fig. 3A). Intriguingly, the addition of a VP1 C-terminal 6xHIS tag on this construct reversed the ratio, with the majority of particles found in the C-antigenic conformation. This was also true for both protease-independent VP1-P2A constructs for which only C-antigenic particles were detected. Thus, the addition of a C-terminal tag to VP1 leads to assembly of particles which readily convert to C-antigenicity or never achieve the D-antigenic conformation despite the presence of stabilizing mutations (Fig. 3).

Although low level VP1 expression was seen in the lysates of the 01-3 construct (Fig. 2), no VLPs were detected in the gradient fractions (Fig. 3). In addition, although strong VP1 expression was apparent for the 03-1 construct (Fig. 2) only low levels of assembled VLPs, which were entirely in the C-antigenic conformation, were observed (Fig. 3).

Interestingly, both VP3-P2A constructs produced D-antigen reactive particles with little to no detectable C-antigen, showing that addition of a C-terminal tag to VP3 is not detrimental to the antigenicity of assembled particles, consistent with the data previously reported following expression in insect cells (Xu et al. 2019). These data demonstrate that D-antigenic VLPs can be produced in *Pichia* without the requirement for coexpression of the viral protease, 3CD. The level of D-antigen produced from each construct was quantified by ELISA using BRP as a standard (Fig. 3B). Although D-antigenic particles are assembled in the absence of 3CD,
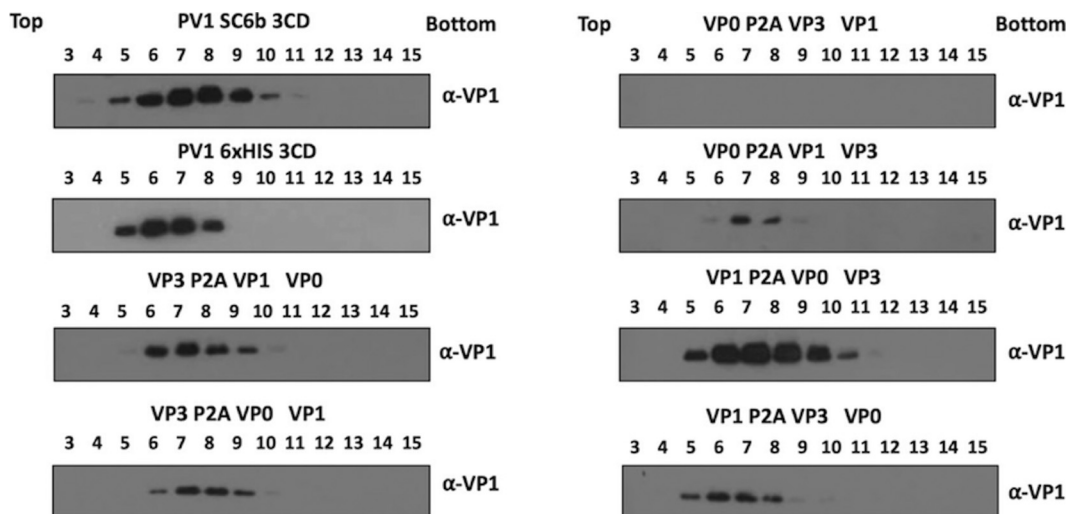
**FIG 2** Gradient purification of protease-dependent and protease-free PV-1 SC6b VLPs. All samples were purified by ultracentrifugation and fractioned from top to bottom in 1 mL aliquots. A 12 $\mu$L sample from each fraction was then taken and boiled in 5x Laemmli buffer and separated by SDS-PAGE prior to analysis by immunoblot using mouse monoclonal $\alpha$-VP1. The figure is a representative example of three separate experiments for each construct.

considerably more was produced in the presence of protease with $\sim$5-fold more D-antigen per 100 mL culture than the 31-0 construct $\sim$3-fold more than the 30-1 construct.

To further characterize the assembled VLPs, peak fractions of the productive constructs were pooled and concentrated using 100 kDa centrifugal concentrators and assessed by immunoblot and ELISA (Fig. 4A and B). The concentrated VLPs were interrogated by immunoblot using a number of different antibodies (Fig. 4A). As expected, the relative levels of VP1 and VP0 were similar for each VLP and only the PV1 SC6b 6xHIS showed reactivity to the anti-HIS antibody. The anti-2A antibody detected the tagged proteins VP3-P2A and VP1-P2A ($\sim$27 kDa and $\sim$33 kDa, respectively) as expected. However, for the VP3-P2A-VP0 VP1 VLPs (30–1), the VP3-P2A band was weaker than that seen with VLPs derived from the 31-0 construct. This may be a consequence of enhanced proteolytic degradation of the 2A tag in the context of the 30-1 VLPs.

We examined the C- and D-antigenic composition of the VLPs in more detail by ELISA following their concentration from the sucrose gradient fractions (Fig. 4B). Both D- and C-antigenic forms were present in VLPs derived from protease-containing constructs, although the D:C ratio was significantly reduced in the P1-6xHIS tagged construct ($P = 0.001$). Little or no D-antigen was detected in the concentrated VP1-P2A VLPs from the VP1-P2A constructs, further indicating that tagged VP1 results in the assembly of C-antigenic VLPs. In contrast, the VLPs, including VP3-2A produced high levels of D-antigenic material and low levels of C-reactivity.

**Protease-independent VLPs maintain classic picornavirus morphology and are thermally stable at physiologically relevant temperatures.** Figure 5A shows representative negative-stain EM images of concentrated protease-independent VLPs and the protease-dependent VLPs. Particles of $\sim$30 nm diameter with typical VLP morphology were seen in all samples, consistent with previous EM images of PV virions and empty capsids and *Pichia*-derived PV-1 VLPs (30). Smaller particles were also seen, especially in the protease-independent samples, which are likely to be *Pichia* alcohol oxidase or fatty acid synthetase which have been shown previously to copurify with VLPs (33). They are likely more frequent in the protease-independent samples, as these required double the yeast culture volume compared to protease-dependent samples, (400 mL versus 200 mL), to provide comparable amounts of antigen. We conducted a size analysis to further compare the VLPs produced from the different constructs (Fig. 5B.). Interestingly, the particles with a higher C:D antigen content, PV1 SC6b 6x HIS 3CD, 13-0, and 10-3, were slightly larger, with statistically significant average sizes of 32.27 nm, 31.95 nm, and 32.11 nm, respectively, compared to PV1 SC6b 3CD particles, which produced particles with an average size
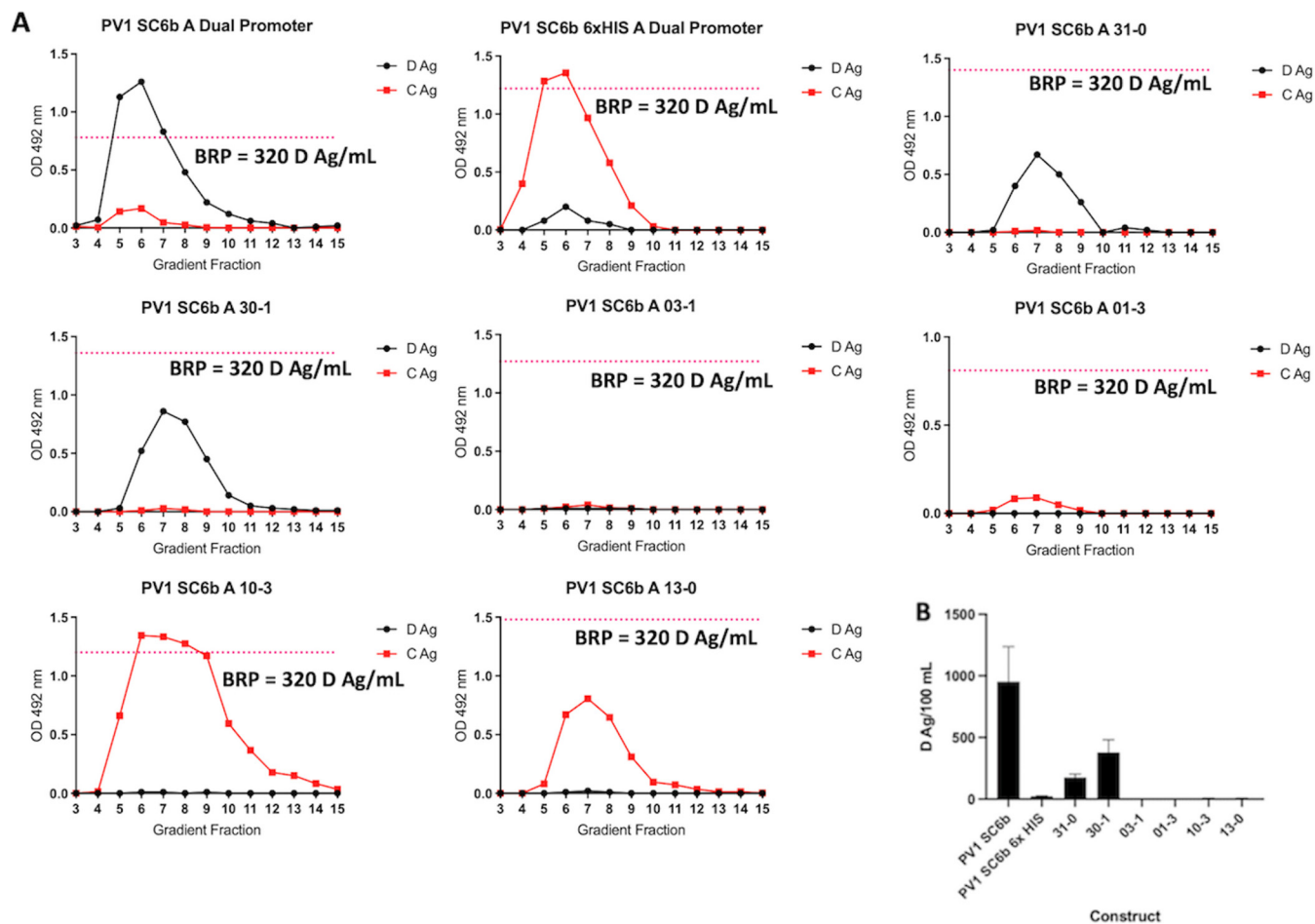
**FIG 3** Antigenicity of PV-1 VLPs. (A) Reactivity of gradient fractions with Mab 234 (D-antigen) and Mab 1588 (C-antigen) in ELISA. The pink dashed line represents the positive control, BRP, for the D-antigen ELISA. OD at $\lambda = 492$ nm is represented in arbitrary units. The figure is a representative example of three separate experiments for each construct. (B) Quantification of D-antigen production per 100 mL of expression culture as determined by ELISA with Mab 234 ($n = 3$). Construct nomenclature is as follows: 31-0 = VP3 P2A VP1 VP0, 30-1 = VP3 P2A VP0 VP1, 03-1 = VP0 P2A VP3 VP1, 01-3 = VP0 P2A VP1 VP3, 10-3 = VP1 P2A VP0 VP3, and 13-0 = VP1 P2A VP3 VP0.

of 31.22 nm. This is consistent with previous studies which showed that the conversion of D-C antigenic particles is associated with an ~3% expansion of the particles (34).

Potential vaccines will need to withstand physiologically relevant temperatures and so the D-antigenicity of VP3-P2A containing VLPs, protease-derived VLPs, and BRP, was assessed following exposure to increasing temperatures (Fig. 5C). The positive control, BRP, was the most thermally stable, only showing a 50% decrease in D-antigenicity at ~50°C, whereas PV-1 SC6b 3CD VLPs lost 50% D Ag ~41°C, although VLPs with VP1 6xHIS were least stable with D-antigenicity dropping sharply above 37°C and retaining only 11% at 40°C. Importantly, both VP3-P2A containing VLPs maintained D-antigenicity above 37°C (62% and 77% for 30-1 VLPs and 31-0 VLPs, respectively). These results suggest that protease-free production of PV VLPs can yield particles which are antigenically stable at physiologically relevant temperatures, suggesting the potential to produce a long-lasting immune protection against PV.

## DISCUSSION

The current PV vaccines require the production of large amounts of infectious virus, with potential to reintroduce the virus to the environment (2, 4). Moreover, continued use of OPV has contributed to the global increase in cVDPV cases, which now exceed those caused by wt PV (7). However, these vaccines are hugely important for eradication of PV, especially in light of the recently licensed nOPV2, which has been intelligently designed to reduce the likelihood of the two major concerns surrounding OPV, reversion and recombination (8).
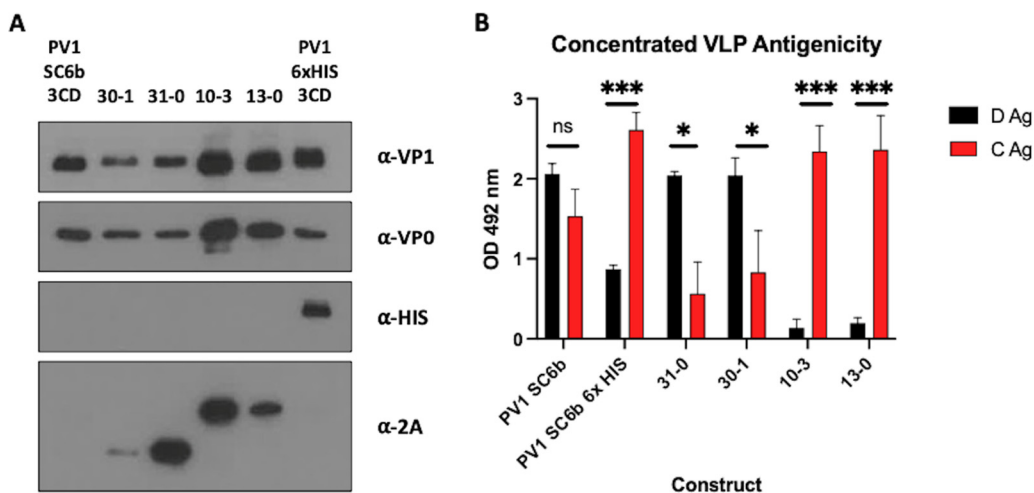
**FIG 4** Characterization of protease-dependent and protease-independent PV-1 SC6b VLPs. (A) Immunoblot for PV VP1, VP0, 6xHIS and 2A peptide. Peak gradient fractions for each VLP preparation were concentrated using 100 kDa microcentrifuge concentrators (Amicon) to ~100 μL. All samples were mixed 1:1 with 2x Laemmli buffer, boiled and separated by SDS-PAGE prior to analysis by immunoblot using mouse monoclonal α-VP1, a rabbit polyclonal α-VP0, mouse monoclonal α-HIS and mouse monoclonal α-2A. (B) Antigenicity of concentrated PV-1 VLPs. Reactivity of concentrated fractions with Mab 234 (D-antigen) and Mab 1588 (C-antigen) in ELISA. OD at $\lambda$ = 492 nm is represented in arbitrary units ($n$ = 3). Means $+/-$ standard deviation. Statistical analysis determined by two-tailed T-test (ns, not significant; *, $P$ value $>$ 0.05, ***, $P$ value $>$ 0.001). Construct nomenclature is as follows: 31-0 = VP3 P2A VP1 VP0, 30-1 = VP3 P2A VP0 VP1, 10-3 = VP1 P2A VP0 VP3 & 13-0 = VP1 P2A VP3 VP0.

With this newly available vaccine, and advances with improved PV-1 and PV-3 OPV vaccines, there is increased optimism that a polio-free world is achievable. However, for the complete elimination of polio alternative PV vaccines which do not require the growth of large quantities of infectious virus for their production still require investigation. VLP vaccines produced using a heterologous expression system may address this requirement. This approach has been successful in a number of expression systems, including plant, insect cell, MVA-based mammalian cell expression systems and, as we show here, yeast systems such as *Pichia pastoris* (24–30, 35). However, the 3C protease, the active component of the P1 cleavage specific precursor 3CD, has been shown to have a toxic effect on cell viability. While 3CD should be less toxic than 3C, it still has the potential for cellular toxicity (12, 31). This may result in reduced yield of VLPs produced in heterologous expression systems, as highlighted by our failure to select viable colonies in *Pichia pastoris* when expressing 3CD under a constitutive promoter. However, a recent publication indicated the potential of protease-independent production of PV VLPs using an insect cell expression system in which the two structural proteins, VP0 and VP3, were separated by inserting a P2A peptide, and with VP1 under the control of a second promoter (28). Here, we explored all permutations of P2A containing protease-independent VLP constructs using *Pichia pastoris* as a heterologous expression system.

We investigated the efficiency of viral capsid protein expression by immunoblot analysis (Fig. 1B.) Good levels of VP1 were produced from both protease-dependent constructs and from each protease-independent construct where the VP1 ORF was located immediately after the promoter, with or without the P2A peptide. However, lower levels of VP1 were seen when the VP1 ORF was placed after the P2A peptide. This suggests that although in the appropriate context the P2A peptide is highly efficient at reinitiating translation following pausing in mammalian cells, the efficiency of this reinitiation event in *Pichia* is lower (36). This also suggests that the individual structural proteins are unlikely to be at equimolar amounts within the cell, which would inevitably reduce capsid assembly efficiency. Therefore, there is potential to improve this process in future either by selection of an alternative 2A peptide or by the expressing all three structural proteins individually from different promoters (37).

Following conformation that each of these constructs produced the viral structural proteins, we compared the production of VLPs from the protease-independent constructs with those from the protease-dependent constructs, which were previously shown to produce
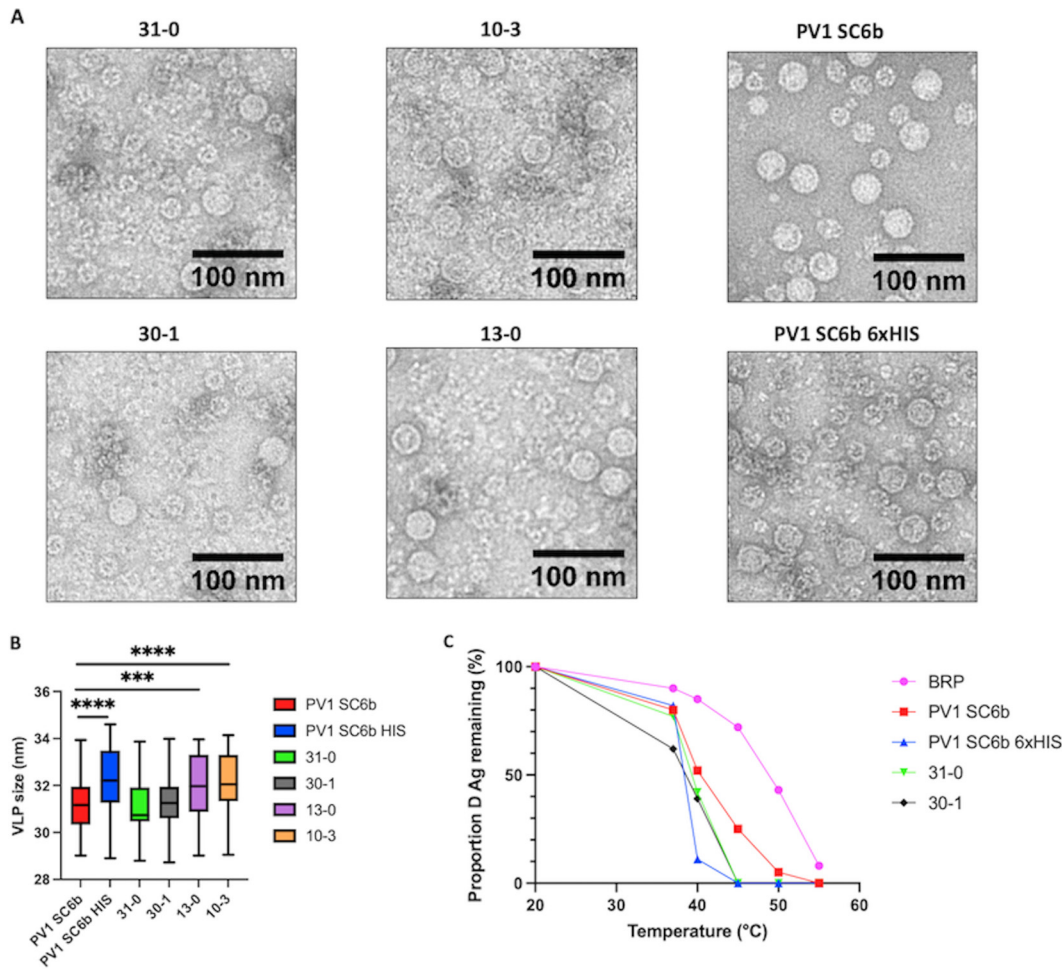
**FIG 5** Transmission electron microscopy of VLPs and thermostability. (A) Representative micrographs of protease-dependent and protease-free PV-1 SC6b VLPs. (Scale bar shows 100 nm). (B) Size analysis of PV VLPs, particles were measured for each construct using ImageJ. ($n = 100$ per construct) Means $+/-$ standard deviation. Statistical analysis determined by two-tailed T-test (***, $P$ value $> 0.001$, ****, $P$ value $> 0.0001$) only statistically significant comparisons are highlighted for clarity. (C) Reactivity of purified PV-1 SC6b VLPs and BRP aliquots to D-antigen specific MAb 234 in ELISA after incubation at different temperatures for 10 min, normalized to corresponding aliquot incubated at 4°C. The figure is a representative example of two separate experiments for each construct. Construct nomenclature is as follows: 31-0 = VP3 P2A VP1 VP0, 30-1 = VP3 P2A VP0 VP1, 10-3 = VP1 P2A VP0 VP3 & 13-0 = VP1 P2A VP3 VP0.

VLPs in *Pichia* (30). Interestingly, almost all of the protease-independent constructs produced material, which sedimented in gradients similarly to VLPs produced from the protease-de-pendent constructs. The exceptions were 03-1 and the 01–3 constructs which produced less material than other protease-dependent and protease-independent constructs (Fig. 2.) Using conformation-specific antibodies in ELISAs of sucrose gradient fractions we saw no signal from the 03-1 construct as expected, and only low levels of C-antigenic and no D-antigenic reactiv-ity from the 01–3 construct. These results suggest that addition of the P2A peptide to the C-terminal end of VP0 has detrimental effects on particle assembly.

While VP1-P2A tagged constructs produced assembled VLPs, as demonstrated by su-crose gradient centrifugation analyses (Fig. 2.) and morphologically by TEM (Fig. 5A.), these were entirely in the C-antigenic conformation (Fig. 3 and 4A). This was dominance of the C-antigenic conformation was also seen when a C-terminal 6xHIS tag added to VP1 in the protease-dependent construct, although some D-antigenicity was detected. Virus particles with 2A peptide still attached have been previously described for foot-and-mouth disease virus, another member of the picornavirus family, although the par-ticle expansion and antigenic conformational changes seen with PV are not observed here (38). However, in closer relatives to PV, VP1 C-terminal extensions which include a motif

integral to the viral entry process have been found in Coxsackieviruses, echoviruses and human parechoviruses (39–41).

Interestingly, both VP3-P2A constructs produced D-antigenic VLPs, in agreement with previous work in insect cells, which showed that a dual promoter construct containing VP3-P2A-VP0 under the control of one promoter and VP1 under the control of a second promoter produced D-antigenic VLPs (28.) Our initial sucrose gradient analyses (Fig. 2.) suggested that these constructs produced little to no detectable C-antigenicity, while maintaining good levels of D-antigenicity. C-antigenicity was detectable after concentration of the VLPs, although at a significantly lower level than D-antigenicity and both constructs produced similar D:C ratios (Fig. 4B.) Intriguingly, when we assessed the levels of P2A peptide in the concentrated VLP samples, the 30-1 VLPs showed less reactivity to the 2A antibody than the 31-0 VLPs, suggesting that the 2A peptide was degraded or cleaved by host factors on these VLPs but not those derived from 31-0, indicating subtle differences in processing of these VLPs, despite the similarity in production. This difference in particle composition may also account for the small differences seen in thermostability, as the 30-1 VLPs appeared less thermally stable at 37°C, maintaining 62% D-antigenicity, whereas the 31-0 VLPs maintained 77% D-antigenicity (Fig. 5C).

Importantly, the thermostabilities of the protease-independent VLPs were similar to those of the protease-dependent PV1 SC6b VLPs and maintained D-antigenicity at physiologically relevant temperatures. These properties suggest that the protease-independent VLPs have the potential to induce protective immune responses against PV. However, the yields of protease-independent VLPs were lower than protease-dependent VLPs, likely due to inefficiency of the P2A translation reinitiation in *Pichia* as highlighted in Fig. 1B. This inefficiency of reinitiation may be addressable by manipulating the sequence surrounding the 2A peptide. In addition, the demonstration that D-antigenic VLPs can be produced using protease-independent means may make these constructs more amenable from a genetic complexity perspective for adaptation to the new vaccine technologies, such as adenovirus-vectored vaccines and mRNA vaccines, which have emerged in response to the SARS-CoV-2 pandemic. They would also circumvent potential problems of cytotoxicity associated with 3CD and facilitate the production of immunogenic enterovirus VLPs *in vivo* (42–44).

In conclusion, we have shown protease-independent production of VLPs using a heterologous expression system, which maintain the antigenic, morphological and thermostability characteristics known to be important drivers of protective immunity against PV. Additionally, our data corroborate the results observed in other expression systems using this thermostable mutant, while building on this work to highlight that VP3 is the only structural protein able to tolerate the addition of a C-terminal P2A tag without negatively impacting assembly or antigenicity. Overall, the protease-independent VLP system we describe provides a framework for the production of VLPs using modern vaccine technologies, not only for PV but also as a model system for other members of the picornavirus family.

## MATERIALS AND METHODS

**Vector construction.** The P1 gene of PV1 SC6b Mahoney was amplified from a pT7RbzMahSC6bP1_deletion mutant plasmid sourced from NIBSC, UK and a 3CD gene was codon optimized for expression in *Pichia pastoris*. Both P1 genes and the 3CD were cloned separately into the pPink-HC expression vector multiple cloning site (MCS) using EcoRI and FseI (NEB). Subsequently, the dual promoter expression vector was constructed through PCR amplification from position 1 of the 3CD pPink-HC to position 1285 inserting a SacII restriction site at both the 5′ and 3′ end of the product. The P1 expression plasmids were linearized by SacII (NEB), followed by the insertion of the 3CD PCR product into SacII-linearized P1 plasmid. All PCR steps were carried out with Phusion polymerase (NEB) using the manufacturer's guidelines. The PV1 SC6b 6xHIS P1 construct was subcloned by the addition of the 6xHIS tag through PCR amplification of the PV1 SC6b P1 from the PV1 SC6b P1 pPink-HC vector. The PV1 SC6b 6xHIS P1dual promoter expression vector was then constructed as described above. The PV1 SC6b P1 pPink-HC vector was used as the template to produce each porcine teschovirus 2A (P2A) containing construct. P2A was inserted into each construct through overlap PCR amplification and then dual promoter expression constructs for each P2A construct were obtained as described above for the 3CD containing plasmids. Each construct was validated by Sanger sequencing provided by Genewiz (Azenta), United Kingdom.

**Yeast transformation and induction.** Plasmids were linearized by AflII digestion (NEB) and then transformed into PichiaPink Strain one (Invitrogen, USA) by electroporation as per the manufacturer's guidelines. Transformed yeast cells were plated on *Pichia* Adenine Dropout (PAD) selection plates and incubated at

28°C until sufficient numbers of white colonies appeared (3 to 5 days). To screen for high-expression clones, 8 colonies were randomly selected for small-scale (5 mL) expression experiments. Briefly, colonies were cultured in YPD for 48 h at 28°C and after shaking at 250 rpm, each culture was pelleted at $1500 \times g$ and resuspended in YPM (1 mL & methanol 0.5% vol/vol) to induce protein expression and cultured for a further 48 h. Cultures were fed methanol to 0.5% vol/vol 24 h postinduction. Expression levels of each clone were determined through VP1 expression analyzed by immunoblotting as described below. For VLP production, a stab from a previously high-expressing glycerol stock was cultured for 48 h in 5 mL YPD to high density. To increase biomass for the protease containing constructs, 4 mL of the starter culture was added to 200 mL YPD in a 2 L baffled flask and cultured at 28°C at 250 rpm for a further 24 h. Cells were pelleted at $1500 \times g$ and resuspended in 200 mL YPM (methanol 0.5% vol/vol) and cultured for a further 48 h. Cultures were fed methanol to 0.5% vol/vol 24 h postinduction. For 2A containing constructs, the cultures were produced in the same way but in a total volume of 400 mL per construct. After 48 h cells were pelleted at $2000 \times g$ and resuspended in breaking buffer (50 mM sodium phosphate, 5% glycerol, 1 mM EDTA, pH 7.4) and frozen prior to processing.

**Purification and concentration of PV and PV VLPs.** *Pichia* cell suspensions were thawed and subjected to cell lysis using CF-1 cell disruptor at $\sim$275 MPa chilled to 4°C following the addition of 0.1% Triton X-100. The resulting lysate was then centrifuged at 5000 rpm to remove the larger cell debris, followed by a $10,000 \times g$ spin to remove further insoluble material. The supernatant was then nuclease treated using 25 U/mL DENARASE (c-LEcta) for 1.5 h at RT with gentle agitation. The supernatant was then mixed with PEG 8000 (20% vol/vol) to a final concentration of 8% (vol/vol) and incubated at 4°C overnight. The precipitated protein was pelleted at 5,000 rpm and resuspended in PBS. The solution was then pelleted again at 5,000 rpm and the supernatant collected for a subsequent $10,000 \times g$ spin to remove any insoluble material. The supernatant was collected and pelleted through a 30% (wt/vol) sucrose cushion at $151,000 \times g$ (using a Beckman SW 32 Ti rotor) for 3.5 h at 10°C. The resulting pellet was resuspended in PBS + NP-40 (1% vol/vol) + sodium deoxycholate (0.5% vol/vol) and clarified by centrifugation at $10,000 \times g$. Supernatant was purified through 15 to 45% (wt/vol) sucrose density gradient by ultracentrifugation at $151,000 \times g$ (using a 17 mL Beckman SW32.1 Ti rotor) for 3 h at 10°C (16). Gradients were collected in 1 mL fractions from top to bottom and analyzed for the presence of VLPs through immunoblotting and ELISA. For electron microscopy and thermostability studies, peak fractions from primary gradients were diluted and purified through a second 15 to 45% (wt/vol) sucrose density gradient by ultracentrifugation at $151,000 \times g$ for 3 h at 10°C.

Peak gradient fractions as determined by immunoblotting and ELISA were then concentrated to $\sim$100 $\mu$L in PBS + 20 mM EDTA using 0.5 mL 100 kDa centrifugal concentration columns (Amicon) as per the manufacturer's instructions.

**Sample preparation and immunoblotting.** Gradient fraction samples were mixed 5:1 with 5$\times$ Laemmli buffer and analyzed by 12% SDS-PAGE (wt/vol) using standard protocols. Concentrated VLP samples were prepared at a 1:1 ratio using 2$\times$ Laemmli buffer. Immunoblot analyses were performed using a monoclonal blend primary antibody against VP1 protein of each PV1, PV2, and PV3 (Millipore MAB8655) followed by detection with a goat anti-mouse secondary antibody conjugated to horseradish peroxidase and developed using the chemiluminescent substrate (Promega). To detect VP0, a rabbit polyclonal antibody was used followed by detection with a goat anti-rabbit secondary antibody conjugated to horseradish peroxidase and developed using a chemiluminescent substrate (Promega). Immunoblot detection of 6xHIS and 2A peptide tags were determined through anti-Histidine tag (AD1.1.10, Bio-Rad) and anti-2A peptide (3H4, Novus Biologicals), followed by detection with a goat anti-mouse secondary antibody conjugated to horseradish peroxidase, and developed using the chemiluminescent substrate (Promega) (45).

**Enzyme-linked immunosorbent assay (ELISA).** To determine the antigenic content of gradient fractions a noncompetitive sandwich ELISA was used to measure PV1 D- and C-antigen content (46). Briefly, 2-fold dilutions of antigen were captured using a PV1-specific polyclonal antibody, and then detected using anti-PV1 d-antigen (Mab 234) or C-antigen (Mab 1588) specific monoclonal antibodies (kindly provided by NIBSC), followed by anti-mouse peroxidase conjugate (47, 48). All ELISAs were then analyzed through Biotek PowerWave XS2 plate reader.

**Thermostability assay.** The thermostability of VLPs was assessed using previously published protocols (32). Briefly, quantified PV VLPs were diluted in phosphate-buffered saline (Corning 46-013-CM) to provide a uniform quantity of D-antigen. Duplicate aliquots were incubated on ice (control) or in a thermocycler (BIO-RAD T100) at temperatures between 20°C and 60°C for 10 min.

Thermostability of the VLPs was assessed by measuring loss of D-antigenicity by ELISA, detection of d-antigenic particles was determined through PV-1 specific Mab 234.

**Electron microscopy.** To prepare samples for negative stain transmission EM, carbon-coated 300-mesh copper grids were glow-discharged in air at 10 mA for 30 s. 3 $\mu$L aliquots of purified VLP stocks were applied to the grids for 30 s, then excess liquid was removed by blotting. Grids were washed twice with 10 $\mu$L distilled H2O. Grids were stained with 10 $\mu$L 1% uranyl acetate solution, which was promptly removed by blotting before another application of 10 $\mu$L 1% uranyl acetate solution for 30 s. Grids were subsequently blotted to leave a thin film of stain, then air-dried. EM was performed using an FEI Tecnai G2-Spirit transmission electron microscope (operating at 120 kV with a field emission gun) with a Gatan Ultra Scan 4000 CCD camera (ABSL, University of Leeds).

**Image processing.** Raw micrographs were visualized with ImageJ 1.51d. Particle sizes were determined using ImageJ analysis software (49, 50).

**Statistical analysis.** All t-tests were two-tailed and performed using the statistical analysis software Prism.

## SUPPLEMENTAL MATERIAL

Supplemental material is available online only.

**SUPPLEMENTAL FILE 1**, PDF file, 0.1 MB.

## ACKNOWLEDGMENTS

## REFERENCES

1. Polio Now–GPEI. https://polioeradication.org/polio-today/polio-now/. Accessed 15 March 2022.
2. Zambon M, Martin J. 2018. Polio eradication: next steps and future challenges. Eurosurveillance 23. https://doi.org/10.2807/1560-7917.ES.2018.23.47.1800625.
3. Two out of three wild poliovirus strains eradicated. https://www.who.int/news-room/feature-stories/detail/two-out-of-three-wild-poliovirus-strains-eradicated. Accessed 22 April 2022.
4. Bandyopadhyay AS, Garon J, Seib K, Orenstein WA. 2015. Polio vaccination: past, present and future. Future Microbiol 10:791–808. https://doi.org/10.2217/fmb.15.19.
5. Minor P. 2009. Vaccine-derived poliovirus (VDPV): impact on poliomyelitis eradication. Vaccine 27:2649–2652. https://doi.org/10.1016/j.vaccine.2009.02.071.
6. Jegouic S, Joffret M-L, Blanchard C, Riquet FB, Perret C, Pelletier I, Colbere-Garapin F, Rakoto-Andrianarivelo M, Delpeyroux F. 2009. Recombination between polioviruses and co-circulating coxsackie A viruses: role in the emergence of pathogenic vaccine-derived polioviruses. PLoS Pathog 5:e1000412. https://doi.org/10.1371/journal.ppat.1000412.
7. Greene SA, Ahmed J, Datta SD, Burns CC, Quddus A, Vertefeuille JF, Wassilak SGF. 2019. Progress toward polio eradication—Worldwide, January 2017–March 2019. MMWR Morb Mortal Wkly Rep 68:458–462. https://doi.org/10.15585/mmwr.mm6820a3.
8. Te Yeh M, Bujaki E, Dolan PT, Smith M, Wahid R, Konz J, Weiner AJ, Bandyopadhyay AS, Van Damme P, De Coster I, Revets H, Macadam A, Andino R. 2020. Engineering the live-attenuated polio vaccine to prevent reversion to virulence. Cell Host Microbe 27:736–751.e8. https://doi.org/10.1016/j.chom.2020.04.003.
9. Lulla V, Dinan AM, Hosmillo M, Chaudhry Y, Sherry L, Irigoyen N, Nayak KM, Stonehouse NJ, Zilbauer M, Goodfellow I, Firth AE. 2019. An upstream protein-coding region in enteroviruses modulates virus infection in gut epithelial cells. Nat Microbiol 4:280–292. https://doi.org/10.1038/s41564-018-0297-1.
10. Tuthill TJ, Groppelli E, Hogle JM, Rowlands DJ. 2010. Picornaviruses, p 43–89. In Current topics in microbiology and immunology.
11. Molla A, Harris KS, Paul AV, Shin SH, Mugavero J, Wimmer E. 1994. Stimulation of poliovirus proteinase 3Cpro-related proteolysis by the genome-linked protein VPg and its precursor 3AB. J Biol Chem 269:27015–27020. https://doi.org/10.1016/S0021-9258(18)47119-0.
12. Jore J, De Geus B, Jackson RJ, Pouwels PH, Enger-Valk BE. 1988. Poliovirus protein 3CD is the active protease for processing of the precursor protein P1 in vitro. J Gen Virol 69:1627–1636. https://doi.org/10.1099/0022-1317-69-7-1627.
13. Kräusslich HG, Nicklin MJ, Lee CK, Wimmer E. 1988. Polyprotein processing in picornavirus replication. Biochimie 70:119–130. https://doi.org/10.1016/0300-9084(88)90166-6.
14. Jiang P, Liu Y, Ma H-C, Paul AV, Wimmer E. 2014. Picornavirus morphogenesis. Microbiol Mol Biol Rev 78:418–437. https://doi.org/10.1128/MMBR.00012-14.
15. Hogle JM, Chow M, Filman DJ. 1985. Three-dimensional structure of poliovirus at 2.9 A resolution. Science 229:1358–1365. https://doi.org/10.1126/science.2994218.
16. Basavappa R, Filman DJ, Syed R, Flore O, Icenogle JP, Hogle JM. 1994. Role and mechanism of the maturation cleavage of VP0 in poliovirus assembly: structure of the empty capsid assembly intermediate at 2.9 Å resolution. Protein Sci 3:1651–1669. https://doi.org/10.1002/pro.5560031005.
17. Le Bouvier GL. 1955. The modification of poliovirus antigens by heat and ultraviolet light. Lancet 269:1013–1016. https://doi.org/10.1016/s0140-6736(55)93435-8.
18. Le Bouvier GL. 1959. Poliovirus D and C antigens: their differentiation and measurement by precipitation in agar. Br J Exp Pathol 40:452–463.
19. Beale AJ, Mason PJ. 1962. The measurement of the D-antigen in poliovirus preparations. J Hyg (Lond) 60:113–121. https://doi.org/10.1017/s002217240003936x.
20. McAleer WJ, Buynak EB, Maigetter RZ, Wampler DE, Miller WJ, Hilleman MR. 1984. Human hepatitis B vaccine from recombinant yeast. Nature 307:178–180. https://doi.org/10.1038/307178a0.
21. Sasagawa T, Pushko P, Steers G, Gschmeissner SE, Hajibagheri MA, Finch J, Crawford L, Tommasino M. 1995. Synthesis and assembly of virus-like particles of human papillomaviruses type 6 and type 16 in fission yeast Schizosaccharomyces pombe. Virology 206:126–135. https://doi.org/10.1016/s0042-6822(95)80027-1.
22. Smith J, Lipsitch M, Almond JW. 2011. Vaccine production, distribution, access, and uptake. Lancet 378:428–438. https://doi.org/10.1016/S0140-6736(11)60478-9.
23. Rombaut B, Jore JP. 1997. Immunogenic, non-infectious polio subviral particles synthesized in Saccharomyces cerevisiae. J Gen Virol 78:1829–1832. https://doi.org/10.1099/0022-1317-78-8-1829.
24. Ansardi DC, Porter DC, Morrow CD. 1991. Coinfection with recombinant vaccinia viruses expressing poliovirus P1 and P3 proteins results in polyprotein processing and formation of empty capsid structures. J Virol 65:2088–2092. https://doi.org/10.1128/JVI.65.4.2088-2092.1991.
25. Viktorova EG, Khattar SK, Kouiavskaia D, Laassri M, Zagorodnyaya T, Dragunsky E, Samal S, Chumakov K, Belov GA. 2018. Newcastle disease virus-based vectored vaccine against poliomyelitis. J Virol 92. https://doi.org/10.1128/JVI.00976-18.
26. Bahar MW, Porta C, Fox H, Macadam AJ, Fry EE, Stuart DI. 2021. Mammalian expression of virus-like particles as a proof of principle for next generation polio vaccines. NPJ Vaccines 6:5. https://doi.org/10.1038/s41541-020-00267-3.
27. Bräutigam S, Snezhkov E, Bishop DHL. 1993. Formation of poliovirus-like particles by recombinant baculoviruses expressing the individual VP0, VP3, and VP1 proteins by comparison to particles derived from the expressed poliovirus polyprotein. Virology 192:512–524. https://doi.org/10.1006/viro.1993.1067.
28. Xu Y, Ma S, Huang Y, Chen F, Chen L, Ding D, Zheng Y, Li H, Xiao J, Feng J, Peng T. 2019. Virus-like particle vaccines for poliovirus types 1, 2, and 3 with enhanced thermostability expressed in insect cells. Vaccine 37:2340–2347. https://doi.org/10.1016/j.vaccine.2019.03.031.
29. Marsian J, Fox H, Bahar MW, Kotecha A, Fry EE, Stuart DI, Macadam AJ, Rowlands DJ, Lomonossoff GP. 2017. Plant-made polio type 3 stabilized VLPs—a candidate synthetic polio vaccine. Nat Commun 8:245. https://doi.org/10.1038/s41467-017-00090-w.
30. Sherry L, Grehan K, Snowden JS, Knight ML, Adeyemi OO, Rowlands DJ, Stonehouse NJ. 2020. Comparative molecular biology approaches for the production of poliovirus virus-like particles using Pichia pastoris. mSphere 5:e00838–19. https://doi.org/10.1128/mSphere.00838-19.
31. Barco A, Feduchi E, Carrasco L. 2000. Poliovirus protease 3Cpro kills cells by apoptosis. Virology 266:352–360. https://doi.org/10.1006/viro.1999.0043.
32. Fox H, Knowlson S, Minor PD, Macadam AJ. 2017. Genetically thermo-stabilised, immunogenic poliovirus empty capsids; a strategy for non-replicating vaccines. PLoS Pathog 13:e1006117. https://doi.org/10.1371/journal.ppat.1006117.

33. Snowden JS, Alzahrani J, Sherry L, Stacey M, Rowlands DJ, Ranson NA, Stonehouse NJ. 2021. Structural insight into Pichia pastoris fatty acid synthase. Sci Rep 11. https://doi.org/10.1038/s41598-021-89196-2.

34. Strauss M, Schotte L, Karunatilaka KS, Filman DJ, Hogle JM. 2017. Cryo-electron microscopy structures of expanded poliovirus with VHHs sample the conformational repertoire of the expanded state. J Virol 91. https://doi.org/10.1128/JVI.01443-16.

35. Lua LHL, Connors NK, Sainsbury F, Chuan YP, Wibowo N, Middelberg APJ. 2014. Bioengineering virus-like particles as vaccines. Biotechnol Bioeng 111:425–440.

36. Kim JH, Lee S-R, Li L-H, Park H-J, Park J-H, Lee KY, Kim M-K, Shin BA, Choi S-Y. 2011. High cleavage efficiency of a 2A peptide derived from porcine teschovirus-1 in human cell lines, zebrafish and mice. PLoS One 6:e18556. https://doi.org/10.1371/journal.pone.0018556.

37. Liu Z, Chen O, Wall JBJ, Zheng M, Zhou Y, Wang L, Ruth Vaseghi H, Qian L, Liu J. 2017. Systematic comparison of 2A peptides for cloning multi-genes in a polycistronic vector. Sci Rep 7:1–9. https://doi.org/10.1038/s41598-017-02460-2.

38. Gullberg M, Polacek C, Bøtner A, Belsham GJ. 2013. Processing of the VP1/2A junction is not necessary for production of foot-and-mouth disease virus empty capsids and infectious viruses: characterization of "self-tagged" particles. J Virol 87:11591–11603. https://doi.org/10.1128/JVI.01863-13.

39. Triantafilou K, Triantafilou M, Takada Y, Fernandez N. 2000. Human parechovirus 1 utilizes integrins $\alpha v\beta 3$ and $\alpha v\beta 1$ as receptors. J Virol 74:5856–5862. https://doi.org/10.1128/jvi.74.13.5856-5862.2000.

40. Zimmermann H, Eggers HJ, Nelsen-Salz B. 1997. Cell attachment and mouse virulence of echovirus 9 correlate with an RGD motif in the capsid protein VP1. Virology 233:149–156. https://doi.org/10.1006/viro.1997.8601.

41. Shakeel S, Seitsonen JJT, Kajander T, Laurinmäki P, Hyypiä T, Susi P, Butcher SJ. 2013. Structural and functional analysis of coxsackievirus A9 integrin $\alpha v\beta 6$ binding and uncoating. J Virol 87:3943–3951. https://doi.org/10.1128/JVI.02989-12.

42. Walsh EE, Frenck RW, Falsey AR, Kitchin N, Absalon J, Gurtman A, Lockhart S, Neuzil K, Mulligan MJ, Bailey R, Swanson KA, Li P, Koury K, Kalina W, Cooper D, Fontes-Garfias C, Shi P-Y, Türeci Ö, Tompkins KR, Lyke KE, Raabe V, Dormitzer PR, Jansen KU, Şahin U, Gruber WC. 2020. Safety and immunogenicity of two RNA-based Covid-19 vaccine candidates. N Engl J Med 383:2439–2450. https://doi.org/10.1056/NEJMoa2027906.

43. Folegatti PM, Ewer KJ, Aley PK, Angus B, Becker S, Belij-Rammerstorfer S, Bellamy D, Bibi S, Bittaye M, Clutterbuck EA, Dold C, Faust SN, Finn A, Flaxman AL, Hallis B, Heath P, Jenkin D, Lazarus R, Makinson R, Minassian AM, Pollock KM, Ramasamy M, Robinson H, Snape M, Tarrant R, Voysey M, Green C, Douglas AD, Hill AVS, Lambe T, Gilbert SC, Pollard AJ, Aboagye J, Adams K, Ali A, Allen E, Allison JL, Anslow R, Arbe-Barnes EH, Babbage G, Baillie K, Baker M, Baker N, Baker P, Baleanu I, Ballaminut J, Barnes E, Barrett J, Bates L, Batten A, Oxford COVID Vaccine Trial Group, et al. 2020. Safety and immunogenicity of the ChAdOx1 nCoV-19 vaccine against SARS-CoV-2: a preliminary report of a phase 1/2, single-blind, randomised controlled trial. Lancet 396:467–478. https://doi.org/10.1016/S0140-6736(20)31604-4.

44. Corbett KS, Edwards DK, Leist SR, Abiona OM, Boyoglu-Barnum S, Gillespie RA, Himansu S, Schäfer A, Ziwawo CT, DiPiazza AT, Dinnon KH, Elbashir SM, Shaw CA, Woods A, Fritch EJ, Martinez DR, Bock KW, Minai M, Nagata BM, Hutchinson GB, Wu K, Henry C, Bahl K, Garcia-Dominguez D, Ma LZ, Renzi I, Kong WP, Schmidt SD, Wang L, Zhang Y, Phung E, Chang LA, Loomis RJ, Altaras NE, Narayanan E, Metkar M, Presnyak V, Liu C, Louder MK, Shi W, Leung K, Yang ES, West A, Gully KL, Stevens LJ, Wang N, Wrapp D, Doria-Rose NA, Stewart-Jones G, Bennett H, et al. 2020. SARS-CoV-2 mRNA vaccine design enabled by prototype pathogen preparedness. Nature 586:567–571. https://doi.org/10.1038/s41586-020-2622-0.

45. Yang P-C, Mahmood T. 2012. Western blot: technique, theory, and trouble shooting. N Am J Med Sci 4:429–434. https://doi.org/10.4103/1947-2714.100998.

46. Singer C, Knauert F, Bushar G, Klutch M, Lundquist R, Quinnan GV. 1989. Quantitation of poliovirus antigens in inactivated viral vaccines by enzyme-linked immunosorbent assay using animal sera and monoclonal antibodies. J Biol Stand 17:137–150. https://doi.org/10.1016/0092-1157(89)90004-8.

47. Minor PD, Ferguson M, Katrak K, Wood D, John A, Howlett J, Dunn G, Burke K, Almond JW. 1991. Antigenic structure of chimeras of type 1 and type 3 polioviruses involving antigenic sites 2, 3 and 4. J Gen Virol 72:2475–2481. https://doi.org/10.1099/0022-1317-72-10-2475.

48. Ferguson M, Wood DJ, Minor PD. 1993. Antigenic structure of poliovirus in inactivated vaccines. J Gen Virol 74:685–690. https://doi.org/10.1099/0022-1317-74-4-685.

49. Schindelin J, Arganda-Carreras I, Frise E, Kaynig V, Longair M, Pietzsch T, Preibisch S, Rueden C, Saalfeld S, Schmid B, Tinevez J-Y, White DJ, Hartenstein V, Eliceiri K, Tomancak P, Cardona A. 2012. Fiji: an open-source platform for biological-image analysis. Nat Methods 9:676–682. https://doi.org/10.1038/nmeth.2019.

50. Schneider CA, Rasband WS, Eliceiri KW. 2012. NIH Image to ImageJ: 25 years of image analysis. Nat Methods 9:671–675. https://doi.org/10.1038/nmeth.2089.